Structure of the Grafted Polyethylene-Based Palladium Catalysts: WAXS and ASAXS Study

K. Jokela,*,† R. Serimaa,*,† M. Torkkeli,† V. Eteläniemi,† and K. Ekman‡

Department of Physical Sciences, P. O. Box 64, FIN-00014 University of Helsinki, Finland, and Smoptech Ltd., Virusmäentie 65, FIN-20300 Turku, Finland

Received May 29, 2002. Revised Manuscript Received August 21, 2002

Wide and anomalous small-angle X-ray scattering (WAXS, ASAXS) methods were used to study the structure of the grafted polyethylene-based palladium catalysts and to find out how the grafting material, polystyrene, poly(acrylic acid), or poly(4-vinylpyridine), affects the structure of the catalyst. The Pd content of the samples was about 5% and Pd(II) was reduced to Pd(0) using the same reducing agent, HCHO. The starting polyethylene fiber was semicrystalline and this structure was not destroyed in the different preparation processes. Pd salts did not crystallize in the samples and the smallest Pd(II) particles were formed in the poly(4-vinylpyridine) grafted sample. Pd(0) crystallites with the average sizes of 35 and 60 Å were formed in the poly(acrylic acid)- and polystyrene-grafted samples, respectively, after reduction of Pd(II) to Pd(0). The poly(4-vinylpyridine)-grafted reduced sample did not contain Pd(0) crystallites. Pd(0) particles showed a tendency to be smaller than Pd(II) particles. The volume distribution of Pd(0) particles of the polystyrene-grafted sample was heterogeneous and indicated a large population of particles with the radii of 60−250 Å. For the poly(acrylic acid)-grafted sample the volume distribution was bimodal, containing maxima at 17 and 58 Å. The smallest Pd(0) particles were formed in the poly-(4-vinyl pyridine)-grafted sample and the maxima of the distribution were at 9 and 20 Å.

1. Introduction

In the past decades the properties of metal nanoparticles have been widely studied because of their promising applications.[1−3] Their properties are assumed to lie somewhere between those of bulk and metal atoms, because of which they have unique properties, for example, in catalysis.[2,4] One method for controlling the morphology of metal nanoparticles is to use a polymer matrix as a medium for nanoparticle formation. The morphology of metal nanoparticles is interesting from the applications point of view because, for example, the size of the palladium cluster affects the hydrogen sorption properties.[4] In the past years several studies about the properties of metal nanoparticles embedded in a polymer matrix have been published.[5−15] These studies have shown that the polymer matrix and the reducing agent affect the morphology of metal nanoparticles.[10−15]

Our work is concentrated on the structure of the grafted polyethylene- (PE-) based palladium (Pd) catalysts. These fiber catalysts can be used for hydrogenation and esterification processes and they are commercially available from Smoptech.[16−20] These catalysts are highly effective and they have a very low diffusional resistance. They can also be regenerated and reused several times. The catalysts can be prepared using several methods, for example, using different grafting

* To whom correspondence should be addressed.
† University of Helsinki.
‡ Smoptech Ltd.

(1) Aiken, J. D., III; Lin, Y.; Finke, R. G. *J. Mol. Catal. A: Chem.* **1996**, *114*, 29.
(2) Aiken, J. D., III; Finke, R. G. *J. Mol. Catal. A: Chem.* **1999**, *145*, 1.
(3) Schmid, G.; Bäumle, M.; Geerkens, M.; Heim, I.; Osemann, C.; Sawitowski, T. *Chem. Soc. Rev.* **1998**, *28*, 179.
(4) Züttel, A.; Nützenadel, Ch.; Schmid, G.; Chartouni, D.; Schlapbach, L. *J. Alloys Compd.* **1999**, *293−295*, 472.
(5) Kralik, M.; Hronec, M.; Jorik, V.; Lora, S.; Palma, G.; Zecca, M.; Biffis, A.; Corain, B. *J. Mol. Catal. A: Chem.* **1995**, *101*, 143.
(6) Corain, B.; Kralik, M. *J. Mol. Catal. A: Chem.* **2000**, *159*, 153.
(7) Corain, B.; Kralik, M. *J. Mol. Catal. A: Chem.* **2001**, *173*, 99.
(8) Ziegler, S.; Theis, J.; Fritsch, D. *J. Membr. Sci.* **2001**, *187*, 71.
(9) Chen, C.-W.; Chen, M.-Q.; Serizawa, T.; Akashi, M. *Chem. Commun.* **1998**, 831.
(10) Seregina, M. V.; Bronstein, L. M.; Platonova, O. A.; Chernyshov, D. M.; Valetsky, P. M.; Hartmann, J.; Wenz, E.; Antonietti, M. *Chem. Mater.* **1997**, *9*, 923.
(11) Bronstein, L. M.; Platonova, O. A.; Yakunin, A. N.; Yanovskaya, I. M.; Valetsky, P. M.; Dembo, A. T.; Makhaeva, E. E.; Mironov, A. V.; Khokhlov, A. R. *Langmuir* **1998**, *14*, 252.
(12) Svergun, D. I.; Shtykova, E. V.; Dembo, A. T.; Bronstein, L. M.; Platonova, O. A.; Yakuin, A. N.; Valetsky, P. M.; Khokhlov, A. R. *J. Chem. Phys.* **1998**, *109* (24), 11109.
(13) Svergun, D. I.; Shtykova, E. V.; Kozin, M. B.; Volkov, V. V.; Dembo, A. T.; Shtykova Jr., E. V.; Bronstein, L. M.; Platonova, O. A.; Yakunin, A. N.; Valetsky, P. M.; Khokhlov, A. R. *J. Phys. Chem. B* **2000**, *104* (22), 5242.
(14) Svergun, D. I.; Kozin, M. B.; Konarev, P. V.; Shtykova, E. V.; Volkov, V. V.; Chernyshov, D. M.; Valetsky, P. M.; Bronstein, L. M. *Chem. Mater.* **2000**, *12*, 3552.
(15) Chernyshov, D. M.; Bronstein, L. M.; Börner, H.; Berton, B.; Antonietti, M. *Chem. Mater.* **2000**, *12*, 114.
(16) Lindsjö, M. C.; Ekman, K. B.; Näsman, J. H. *J. Polym. Sci., B: Polym. Phys.* **1995**, *33*, 1945.
(17) Kärki, A.; Paatero, E.; Sundell, M. *Ion Exch. Dev. Appl. SCI* **1996**, 486.
(18) Mäki-Arvela, P.; Salmi, T.; Sundell, M.; Ekman, K.; Peltonen, R.; Lehtonen, J. *Appl. Catal., A* **1999**, *184*, 25.
(19) Aumo, J.; Mäki-Arvela, P.; Yu Murzin, D.; Salmi, T.; Ekman, K.; Peltonen, R.; Sundell, M.; Vainio, H. *Chem.-Ing.-Tech.* **2001**, *73* (6), 618.
(20) Lilja, J.; Aumo, J.; Salmi, T.; Murzin, D. Yu.; Mäki-Arvela, P.; Sundell, M.; Ekman, K.; Peltonen, R.; Vainio, H. *Appl. Catal., A* **2002**, *228*, 253.

10.1021/cm0212212 CCC: $22.00
Published on Web 11/07/2002

Table 1. Main Characteristics of the Studied Samples

sample code	grafting material	salt	reducing agent	Pd(II)/Pd(0) content (%) Pd(II)	Pd(0)
PE−PS0	styrene				
PE−PS1		$Pd(NH_3)_4(HCO_3)_2$	-	5	
PE−PS2		$Pd(NH_3)_4(HCO_3)_2$	HCHO		5
PE−PAA0	acrylic acid				
PE−PAA1		$PdCl_2$		5	
PE−PAA2		$PdCl_2$	HCHO		5
PE−P4VP0	4-vinylpyridine				
PE−P4VP1		$PdCl_2$		5	
PE−P4VP2		$PdCl_2$	HCHO		5

materials, Pd salts, and reducing agents. However, the catalytic activity of the materials has varied considerably, indicating that different structures are formed to the catalysts depending on the preparation method.

The aim of this study was to determine the basic structure of the catalysts and to obtain information about the effect of the grafting material on the structure of the catalyst. The Pd content of the samples was similar and Pd(II) was reduced to Pd(0) using the same reducing agent. Wide-angle and anomalous small-angle X-ray scattering (WAXS, ASAXS) methods were used. Both these methods are nondestructive and WAXS was used to study the crystal structure of PE and Pd and ASAXS was used to determine the sizes of Pd particles. With ASAXS the scattering intensity arising from the Pd structures could be separated from the matrix scattering due to the changes in the atomic scattering factor with energy.[22,23] On the basis of the ASAXS results, the volume distribution functions, $D_V(r)$, were calculated.[12]

2. Materials

Polyethylene (PE) fibers were used as a support material for the production of the catalysts. The PE fibers were first irradiated with electrons (200 kGy) and after that grafted using one of the following grafting materials: polystyrene (PS), poly(acrylic acid) (PAA), and poly(4-vinylpyridine) (P4VP). The PS-grafted PE fiber was additionally sulfonated. Pd salt was added to the material (nitrate or chloride). By this procedure three different cation or anion exchangers were formed: the PS-based catalysts were strong, the PAA-based catalysts were weak cation exchangers, and the P4VP-based catalysts were weak anion exchangers. To obtain catalytic active material, Pd was reduced from Pd(II) to Pd(0) using HCHO as a reducing agent. The weight fraction of Pd in the samples was 5%, which was determined using atomic absorption spectroscopy (AAS). The preparation of fiber catalysts (PS-grafted PE fiber) has been described in more detail in refs 18 and 20.

Table 1 summarizes the main characteristics of the studied samples. The starting fiber (PE), the grafted samples (PE−PS0, PE−PAA0, and PE−P4VP0), and the grafted and nonreduced samples (PE−PS1, PE−PAA1, and PE−P4VP1) were studied as reference materials.

3. Experimental Section

3.1. WAXS Measurements. WAXS measurements were made using a Siemens $\theta-2\theta$ diffractometer. The experiments were performed in symmetrical transmission mode with Cu $K\alpha_1$ radiation (1.541 Å), which was monochromatized with a quartz monochromator in the incident beam. The scattered intensities were measured using a scintillation counter and an angular range (2θ) of 30°−90°, an angular step ($\Delta 2\theta$) of 0.2°, and a measurement time of 30 s/point. The measurements were made from the pressed samples. The samples were rotated during the measurements to reduce the effect of the preferred orientation.

The average size of the Pd crystallites was determined from the 111 reflection ($2\theta = 40.2°$ [24]) using the well-known Scherrer formula.[25] The effect of the instrumental broadening on the widths of the reflections was estimated assuming that the shapes of both the true diffraction peak and the instrumental function are Gaussian. The instrumental function was determined by measuring the 111 reflection of the LiF sample ($2\theta = 38.7°$ [24]). The full-width at half-maximum (fwhm) and the positions of the reflections were determined by fitting a Gaussian function to the data. The fwhm of the instrumental function was 0.2°. The accuracy of the crystallite size determination is ±10%.

3.2. ASAXS Measurements. ASAXS measurements were carried out at beamline B1 (JUSIFA) at Hamburger Synchrotronstrahlungslabor (HASYLAB, Germany).[26] The idea of the anomalous scattering experiment is to measure intensity curves of the same sample using several energies of the incident beam, which are chosen close to an absorption edge of the selected element.[27] Then the atomic scattering factor of the selected element,

$$f(k,E) = f_0(k) + f'(E) + if''(E) \quad (1)$$

changes considerably since the anomalous dispersion corrections $f'(E)$ and $f''(E)$ change close to the absorption edges. Far from the absorption edge the scattering factor $f(k,E) \approx f_0(k)$, where $f_0(k)$ is equal to the atomic number of the element on the SAXS region. At the absorption edge $f'(E)$ decreases sharply. $f''(E)$ is small at the energies below the edge but at the edge it jumps sharply. If the measurements are done slightly below the absorption edge, $f''(E)$ is small and thus the imaginary part can be dropped from the analysis.

The measurements were made with energies close to the K absorption edge of Pd, 24.35 keV. The energy range of the measurements was calibrated via an EXAFS measurement of a Pd foil. The EXAFS spectra of some Pd(II) and Pd(0) samples were also measured and the absorption edge of these samples was also at about 24.35 keV, but the shape of the spectra of

(21) Jokela, K.; Serimaa, R.; Eteläniemi, V.; Ekman K.; Honkimäki, V. *J. Polym. Sci. Part B: Polym. Phys.*, submitted.
(22) Haubold, H.-G.; Wang, X. H. *Nucl. Instrum. Methods Phys. Res., Sect. B* **1995**, *97*, 50.
(23) Haubold, H.-G.; Wang, X. H.; Goerigk, G.; Schilling, W. *J. Appl. Crystallogr.* **1997**, *30*, 653.
(24) *Standard X-ray Diffraction Patterns, Vol. 1−10*; National Bureau of Standards, Circular 539, 1952.
(25) Balta-Calleja, F. J.; Vonk, C. G. *X-ray Scattering of Synthetic Polymers*; Elsevier: New York, 1989.
(26) Haubold, H.-G.; Gruenhagen, K.; Wagener, M.; Jungbluth, H.; Heer, H.; Pfeil, A.; Rongen, H.; Brandenburg, B.; Moeller, R.; Matzerarth, J.; Hiller, P.; Halling, H. *Rev. Sci. Instrum.* **1989**, *60*, 1943.
(27) Materlik, G.; Sparks, C. J.; Fisher, C. J. *Resonant Anomalous X-ray Scattering*; Elsevier: New York, 1994.

Pd(II) samples differed from that of Pd(0) samples. The ASAXS measurements from the Pd(0) form samples were made using three different energies: 23.46 keV (E_1), 24.26 keV (E_2), and 24.34 keV (E_3). At these energies $f'(E)$ obtains values of −2.9, −5.0, and −7.2, respectively. The Pd(II) samples were only measured using the energies E_1 and E_3.

The samples were in the vacuum during the measurements. Two different distances between the sample and the detector were used, 3635 and 2737 mm. These distances covered the scattering vector lengths of $0.02 < k < 0.20$ and $0.04 < k < 0.33$ Å^{-1}, respectively. The length of the scattering vector k is defined as $k = 4\pi \sin\theta/\lambda$, where 2θ is the scattering angle and λ is the wavelength. The detector response was studied by measuring the fluorescence yield from a Pd foil. The measured intensities were corrected for the background scattering, the detector response, and the fluoresence intensity and merged to yield the composite curves in the range of $0.02 < k < 0.33$ Å^{-1}. The corresponding Bragg distances were from 19 to 314 Å. The conventional SAXS patterns of the starting fiber and the grafted samples PE−PS0, PE−PAA0, and PE−P4VP0 were also measured using the energy E_3 and the sample-to-detector distance of 3635 mm.

In general, the intensity of the scattering can be expressed as

$$I(k,E) = \sum_{i,j} N_i f_i(k,E) f_j(k,E) S_{ij}(k) \quad (2)$$

where N_i is the number of atoms of element i, f_i is the atomic scattering factor, and S_{ij} is the partial structure factor. In the case of the binary systems (atoms a and b) $I(k,E)$ can be expressed as

$$I(k,E) = N_a |f_a|^2 S_{aa}(k) + N_b |f_b|^2 S_{bb} + 2N_a \mathrm{Re}[f_a f_b^*] S_{ab} \quad (3)$$

All the partial structure factors may be solved from the set of intensity curves if the measurements are done using at least three different energies.[27,28] However, large statistical accuracy is needed and in many cases the mutual correlation term S_{ab} is assumed to be zero to make the analysis easier.

From the ASAXS measurements the difference intensity, $\Delta I_j(k)$, was obtained as

$$\Delta I_j(k) = I(k,E_1) - I(k,E_j) \quad (4)$$

When $f'(E)$ decreases at the absorption edge, the intensity arising from structures containing Pd decreases. If no mutual correlation is assumed, the difference intensity is that intensity, which arises from the structures containing Pd. We used this assumption and verified it by comparing the difference intensity $\Delta I_j(k)$ of one Pd(0) form sample (not included in this study) and the difference intensity calculated from the conventional SAXS measurements made at a home laboratory. The setup is described in ref 29. These two intensity curves did not differ considerably.

To obtain the size of the Pd structures, the volume distribution functions, $D_V(r)$, were calculated from the $\Delta I_3(k)$ and $\Delta I_2(k)$ curves using the GNOM program,[30] assuming that Pd particles form a polydisperse systems of spherical particles. The assumption is based on AFM data.[32] Because the results for $\Delta I_3(k)$ and $\Delta I_2(k)$ were equal, only the $D_V(r)$ functions obtained from the $\Delta I_3(k)$ curve are provided. An estimate of the average particle size was given by the radius of gyration $R_g = \sqrt{3/5}\langle R\rangle$, where $\langle R\rangle$ denotes the radius of the average sphere in the system. The distance range $R_{min} < r < R_{max}$, where the distribution $D_V(r)$ differs from zero, has to be specified prior to the calculations. As these distances were not known in advance, R_{min} was set to 0 and successive runs with different values of R_{max} were made to find its value for each data set.

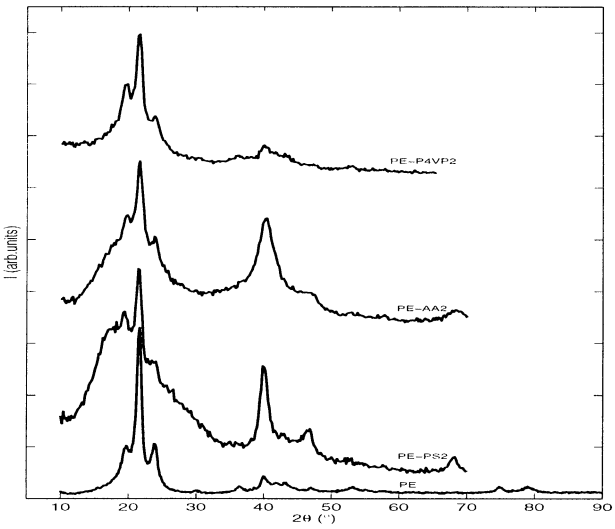

Figure 1. WAXS diffraction patterns of the starting PE fiber and Pd(0) form samples.

4. Results and Discussion

4.1. Starting PE Fiber and Grafted Samples. Figure 1 shows the WAXS diffraction pattern of the starting PE fiber. The pattern is typical for semicrystalline polymer; it includes clearly distinguishable Bragg reflections arising from PE crystallites and an amorphous maximum. The strongest reflections can be identified as arising from the orthorhombic form of PE. The Miller indices of these reflections are 110, 200, 210, 020, 011, and 220 (2θ = 21.7°, 24.2°, 30.3°, 36.5°, 40.0°, and 44.3°, respectively[31]). However, a weak intensity maximum at 19.5° can also be seen. This maximum is reflection 010 of the triclinic form of PE. The average size of PE crystallites, determined from 110 reflection, was 110 Å. The WAXS diffraction patterns of the grafted samples (not shown) include also Bragg reflections arising from PE crystallites, but the amorphous maximum is more pronounced, indicating a decrease in the overall crystallinity.

The SAXS patterns (not shown) of the starting fiber and the grafted samples, measured with Cu Kα using a laboratory setup,[29] showed a maximum arising from lamellar structures and a strong increase toward k = 0. The lamellar period for the starting fiber was 105 Å, which increased due to grafting in the amorphous regions. The upturn of the SAXS intensity toward k = 0 indicated that the fibrous structure is porous, and thus Pd particles can be formed on the surface of the fibers, on the surface of the lamellae within a fiber, and in the amorphous regions between the PE lamellae. SAXS intensities measured at Jusifa showed only a power law behavior arising from increased porosity due to the high vacuum.[33]

4.2. Pd(II) Form Samples. The WAXS patterns of the Pd(II) form samples (not shown) include only the intensity maxima arising from the semicrystalline PE

(28) Haubold, H. G. *J. Phys. IV* **1993**, *C8*, 475.
(29) Jokela, K.; Serimaa, R.; Torkkeli, M.; Sundholm, F.; Kallio, T.; Sundholm, G., *J. Polym. Sci., Part B: Polym. Phys.*, **2002**, *15*, 1539.
(30) Svergun, D. I. *J. Appl. Crystallogr.* **1992** , *25*, 495.
(31) Turley, J. W. *X-ray Diffraction Patterns of Polymers*; International Centre for Diffraction Data, 1994.
(32) Ekman, K. Unpublished results.
(33) Polizzi, S.; Riello, P.; Goerigk, G.; Benedetti, A. *J. Synchrotron. Radiat.* **2002**, *9*, 65.

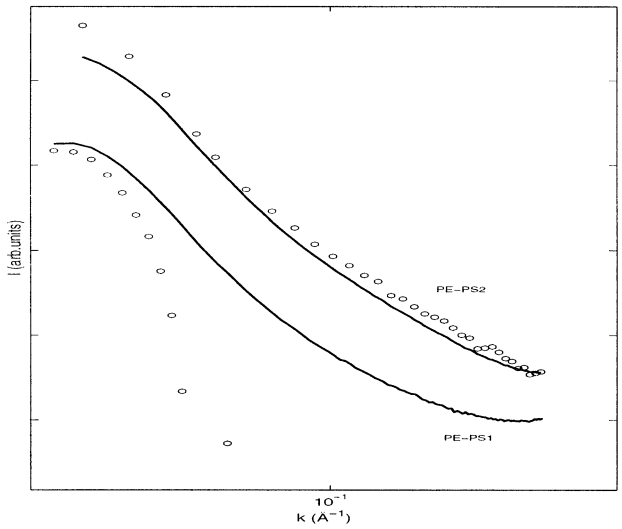

Figure 2. Conventional SAXS (−) and difference ASAXS data $\Delta I_3(k)$ (anomalous signal) (○) of the PS-grafted samples.

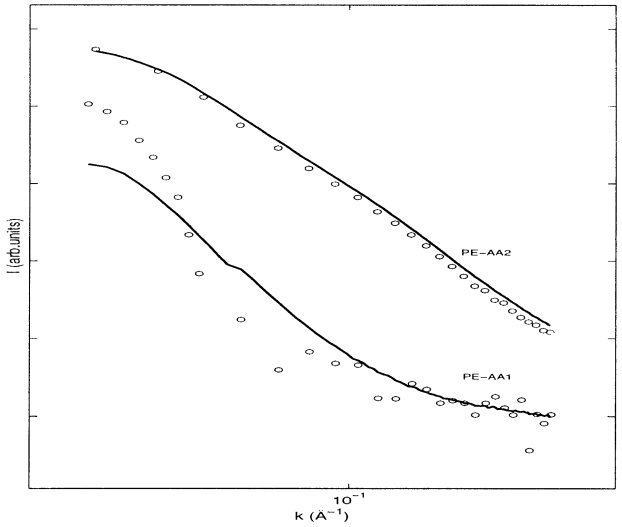

Figure 3. Conventional SAXS (−) and difference ASAXS data $\Delta I_3(k)$ (anomalous signal) (○) of the PAA-grafted samples.

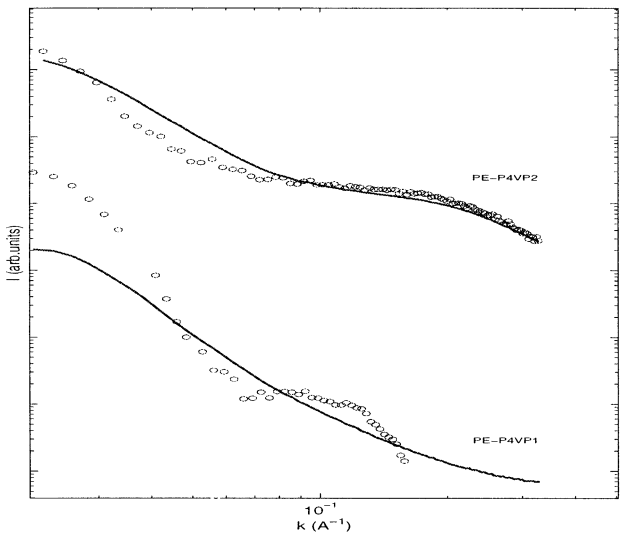

Figure 4. Conventional SAXS (−) and difference ASAXS data $\Delta I_3(k)$ (anomalous signal) (○) of the P4VP-grafted samples.

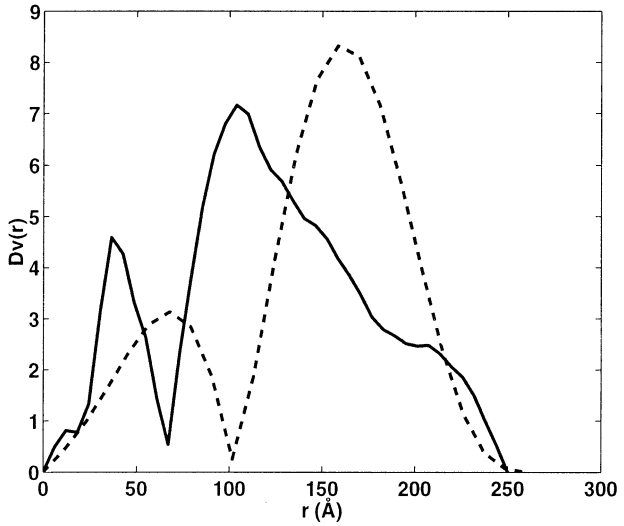

Figure 5. Distribution functions $D_V(r)$ of Pd(II) form samples calculated using the GNOM program. PE−AA1, dashed; PE−P4VP1, solid.

and there are no new diffraction peaks. Thus, when Pd salt was added to the material, it did not form a detectable amount of Pd crystallites and the PE crystallites were not destroyed during the process.

The difference ASAXS curves, $\Delta I_3(k)$, and the conventional SAXS curves, $I(k)$, of the Pd(II) form samples are shown in Figures 2−4. The difference ASAXS curve of the PE−PS1 sample differs markedly from zero only at a very narrow k range close to $k = 0$. This indicates that the size of the Pd(II) particles is large. The difference ASAXS intensity curves of the PE−PAA1 and PE−P4VP1 samples also differ considerably from the conventional SAXS curves being broader than that of PE−PS1. This indicates that the particle size of the PE−PAA1 and PE−P4VP1 samples is smaller than that of the PE−PS1 sample or that Pd(II) is distributed in a different way in the PS-grafted samples than in the PAA- and P4VP-grafted samples.

The difference ASAXS curves of the Pd(II) form samples show the power of the ASAXS method. Svergun et al.[12,13] developed a so-called matrix subtraction procedure to determine the distribution functions of platinum on hydrogel/surfactant complexes by conventional SAXS. However, in our case this Pd(II) is not in crystalline form and does not necessarily form a separate structure. This means that the matrix intensity in the case of Pd(II) form samples may differ from that of the grafted samples and thus the difference SAXS curves cannot be calculated on the basis of the conventional SAXS measurements. For instance, a part of Pd^{2+} ions may coordinate by nitrogen atoms of P4VP.[34] When ASAXS is used, the intensity arising from the Pd(II) structures can be separated realistically from the matrix scattering and information on Pd(II) structures is obtained.

The distributions $D_V(r)$ of PE−PAA1 and PE−P4VP1 are shown in Figure 5. In the case of PE−PS1 sample fitting was not done due to the narrow k range. The R_{max} and R_g values are shown in Table 2. In the case of the PAA-grafted sample the distribution $D_V(r)$ of the Pd(II) particles displays two maxima at 67 and 158 Å. The average R_g is 142 ± 1 Å and R_{max} is about 260 Å. For

(34) Drelinkiewicz, A.; Hasik, M.; Quillard, S.; Paluskiewicz C. *J Mol. Struct.* **1999**, *512*, 205.

Table 2. Average Size of Pd Crystallites Calculated from WAXS Measurements from Reflection 111[a]

sample	crystallite size 111 (Å)	distribution $D_V(r)$ R_{max} (Å)	R_g (Å)
PE−PS1			
PE−PS2	60	245	132 ± 3
PE−PAA1		260	141 ± 7
PE−PAA2	35	130	63 ± 1
PE−P4VP1		250	141 ± 7
PE−P4VP2		100	69 ± 1

[a] The accuracy of the crystallite size determination is ±10%. The table also shows the maximum distance, R_{max}, obtained from the distribution $D_V(r)$.

the P4VP-grafted sample the distribution $D_V(r)$ of the Pd(II) particles contains maxima at 38 and 105 Å, the average R_g is 141 ± 7 Å, and the radii of the Pd(II) particles are <250 Å. This result shows the effect of the grafting material: In the case of the P4VP-grafted sample, on average, smaller Pd(II) particles were formed. However, both samples contain also a portion of quite large particles, with radii between 70 and 250 Å.

4.3. Pd(0) Form Samples. Figure 1 shows the WAXS diffraction patterns of the Pd(0) form samples. New intensity maxima arising from Pd crystallites appeared in the WAXS intensity curves of the PS- and PAA-grafted samples when Pd was reduced to Pd(0) form. The patterns also included reflections of PE, so reduction of Pd(II) to Pd(0) does not destroy PE crystallites. The Miller indices of the strongest Pd reflections are 111 and 200. The reflections of Pd and PE are not overlapped, so they can be separated easily from each other. The average size of the Pd crystallites for the PE−PS2 and PE−PAA2 samples, 60 and 35 Å, respectively (Table 2), were calculated from the 111 reflection of Pd. Thus, PS grafting and/or $Pd(NH_3)_4(HCO_3)_2$ salt produces larger crystallites than PAA grafting and/or $PdCl_2$ salt.

The difference ASAXS curves, $\Delta I_3(k)$, and the conventional SAXS curves, $I(k)$, of the Pd(0) form samples are shown in Figures 2−4. The difference ASAXS curve of PE−PS2 diminishes more slowly at large k than that of PE−PS1. This indicates that the size of Pd(0) particles is smaller than the size of Pd(II) particles. The shapes of the difference ASAXS curves of PE−PS2 and PE−PAA2 do not differ considerably from those of the conventional SAXS curves, while that of PE−P4VP2 does. This may be explained by the crystallization of Pd in PS- and PAA-grafted samples observed by WAXS. Because of Pd crystallites, the contribution of the Pd−Pd structure factor (eq 2) may be large in both the total and the difference intensity curve at this k range.

The distributions $D_V(r)$ of the Pd(0) form samples are shown in Figure 6 and the R_{max} and R_g values are shown in Table 2. The R_{max} values of the reduced samples are smaller than those of the Pd(II) form samples. However, the shapes of the distributions $D_V(r)$ differ from each other. The distribution $D_V(r)$ of the PS-grafted sample is broad and displays maxima at 9, 35, 84, and 165 Å. The sample contains a large population of particles with the radii of 60−250 Å. The distribution $D_V(r)$ of the PAA-grafted sample contains maxima at 17 and 58 Å, and the average R_g is 63 ± 1 Å. The particle sizes are notably smaller than those of PE−PS2. The distribution $D_V(r)$ of the P4VP-grafted sample displays maxima at 9 and 20 Å; the average R_g = 69 ± 1 Å and R_{max} is about 100 Å. However, the particle population is concentrated at radii between 0 and 30 Å.

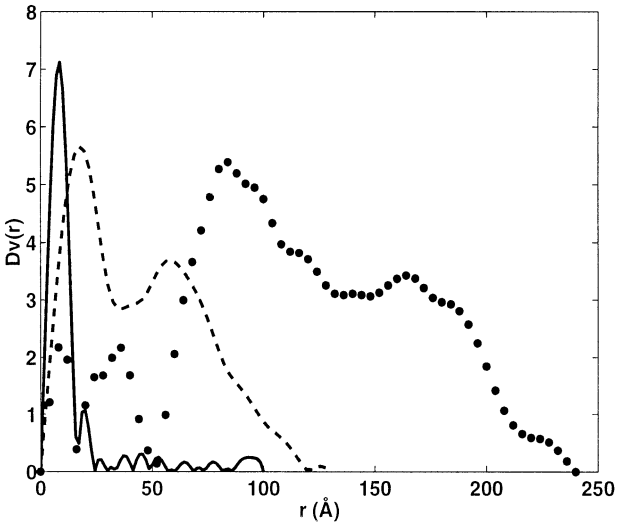

Figure 6. Distribution functions $D_V(r)$ of Pd(0) form samples calculated using the GNOM program. PE−PS2, dotted; PE−AA2, dashed; PE−P4VP2, solid.

The particle sizes are related to the average size of the palladium crystallites—the largest crystallites were formed in the PS-grafted sample and the smallest (=none) in the P4VP-grafted sample. Both in PAA- and PS-grafted samples larger particles are polycrystalline or include weakly ordered regions since the sizes of the crystallites are considerably smaller than the R_{max} values.

5. Conclusions

The basic structure of the grafted PE-based Pd catalysts were determined by WAXS and SAXS. The crystallization of palladium was followed by WAXS and ASAXS gave valuable information on the nanometer-range Pd(II) structures of also those catalyst samples which did not contain Pd(0) crystallites. The starting fiber was semicrystalline and even Pd(0) form samples contained PE crystallites. The diffraction patterns of Pd(II) samples did not include Pd reflections. Pd(II) particles were formed in all the samples and their sizes depended on the grafting material.

Pd(0) crystallites were formed after reduction in the PS- and PAA-grafted samples but not in the P4VP-grafted sample. The Pd(0) particles in the reduced samples were smaller than Pd(II) particles in the nonreduced samples. The largest Pd(0) particles were formed in the PS-grafted sample and the smallest particles in the P4VP-grafted sample. The shapes of the distribution function $D_V(r)$ of the PAA- and P4VP-grafted samples were bimodal while that of the PS-grafted sample contained four separate maxima.

The catalytic activity of the PAA-grafted samples is considerably higher than the catalytic activity of the PS- and P4VP-grafted samples.[32] It was observed that Pd crystallites were formed in both PAA- and PS-grafted catalysts but not in P4VP-grafted catalyst. The lack of crystallites might explain the low activity of P4VP-grafted catalysts. The different activities of the PAA- and PS-grafted samples may be related to the different

size distributions of Pd(0) particles, which affects the size of the active surface of Pd. The choice of the grafting material with a suitable functional group is thus an essential factor determining the particle size. However, as, for example, Seregina et al.[10] have observed for another type of system, the Pd(0) particle distribution can be further controlled by the reducing agent. This will be a topic of future studies.

Acknowledgment. The ASAXS measurements were carried out at the beamline B1 JUSIFA of HASYLAB, Hamburg. The authors gratefully thank the beamline staff, particularly Dr. G. Goerigk for advice concerning data collection and analysis. Financial support from the National Graduate School in Materials Physics (NGSMP) is gratefully acknowledged.

CM0212212